IEEE Access
Multidisciplinary | Rapid Review | Open Access Journal

Received December 5, 2020, accepted December 26, 2020, date of publication December 30, 2020,
date of current version January 12, 2021.

Digital Object Identifier 10.1109/ACCESS.2020.3048127

Novel Adaptive Sparse-Spike Deconvolution Bearing Fault Detection Method Based on Curvelet Transform

YANFENG LI[1], ZHIJIAN WANG[1,2], TIANSHENG ZHAO[3], AND YUAN ZHAO[4]

[1]School of Mechanical Engineering, North University of China, Taiyuan 030051, China
[2]School of Mechanical Engineering, Xi'an Jiaotong University, Xi'an 710049, China
[3]The 713 Research Institute of CSIC, Zhengzhou 450015, China
[4]Taiyuan Research Institute Company Ltd., China Coal Technology and Industry Group, Taiyuan 030006, China

Corresponding author: Zhijian Wang (wangzhijian1013@163.com)

This work was supported in part by the National Natural Science Foundation of China under Grant 51905496.

ABSTRACT This paper has proposed a novel bearing fault detection method about adaptive Sparse-spike Deconvolution based on Curvelet Transform (CTSSD), where the novel technique about adaptive Sparse-spike Deconvolution names after ASSD. Its purpose is to recover the pulse sequence from a vibration signal including complex noise, and to evaluate the periodic pulse position and pulse amplitude. Firstly, in order to make the results sparse and improves the stability of the result, the L1 norm regularization method is proposed in this paper, which is used to constrain the signal pulse sequence sparsely. Secondly, considering that regularization parameters are not adaptive, the Quantum behavior Particle Swarm Optimization (QPSO) algorithm is proposed to determine the optimal regularization parameters, adaptively. Finally, considering that the periodic features of ASSD extraction are not continuous, the Curvelet transform is further introduced. The fault signal is transformed into the Curvelet domain, and the Curvelet coefficient is used to characterize the fault signal pulse sequence. This method proposed in this paper is applied to the simulation signal and the vibration signal of rolling bearing fault, and is compared with the ASSD and the minimum entropy deconvolution (MED) to verify the reliability and effectiveness.

INDEX TERMS Fault diagnosis, Curvelet transform, L1 norm regularization, quantum-behavior particle swarm optimization algorithm.

I. INTRODUCTION

In the development of science and technology nowadays, fault diagnosis is applied to all walks of life. For example, fault diagnosis of modern power grid [1], [2], fault detection of Diesel engine [3] and fault diagnosis of various instruments [4]–[7]. Gearboxes are an indispensable mechanical device in industrial production [8], [9]. In recent years, the fault diagnosis of gearbox has developed rapidly. The fault feature recognition of gearbox mainly includes fault classification [10] and fault feature extraction [11], [12]. Because the rolling bearing is an important part of the gearbox [13], many scholars have done a lot of research on the fault diagnosis of the rolling bearing. When the original component of the rolling bearing fault, the impact periodic signal will be generated, but it's the early fault is very weak [14]. Therefore, under the complex background noise interference, the fault characteristics of the rolling bearing are difficult to detect in time [15].

In recent years, a large number of scholars have made a lot of research for obtaining advanced fault characteristic signal processing technology. For example, Endo and Randall [16] successfully applied Minimum Entropy Deconvolution (MED) to fault detection, MED technology is used to improve the filtering technology based on autoregressive (AR) model, at the same time, the advantages of combining AR filtering and MED filtering in detecting local faults of gearboxes are verified by experiments. Since variational mode decomposition (VMD) can adaptively decompose the vibration signal into multiple intrinsic modes [17], therefore, Liu and Xiang [18] proposed a novel strategy using VMD, L-Kurtosis and minimum entropy deconvolution (MED) to detect mechanical faults. First, the VMD is employed to decompose the raw vibration signal into a set of intrinsic mode functions (IMFs) to eliminate the interference of the noise. Second, the optimal IMF, which contains the

The associate editor coordinating the review of this manuscript and approving it for publication was Zhixiong Peter Li.

faulty information, is determined using L-Kurtosis. Then, the impact characteristic of the periodic impulses in optimal IMF is enhanced through MED. Finally, a Hilbert envelope spectrum analysis is performed to the enhanced signal to extract the faulty feature frequency.

Experiments show that this method can effectively detect mechanical component failure. Wang *et al.* [19] proposed a Maximum Kurtosis Spectrum Entropy Deconvolution (MKSED) method based on MED. It is applied to bearing fault diagnosis. It overcomes the problem that MED is sensitive to the vibration of single abnormal pulse and the problem that the filter length cannot be determined adaptively. However, the MED algorithm uses the kurtosis as the objective function and solves the optimal filter by iteration. Therefore, the shortcoming that only extract a single pulse limits its development. In order to overcome the shortcomings of MED, a method called Maximum Correlation Kurtosis Deconvolution (MCKD) is proposed [20]. Its purpose is to obtain a number of continuous impulse signals by convoluting periodic pulse faults with mechanical vibration signals. A large number of scholars have studied this method. In recent years, for example, Zhang *et al.* [21] proposed a new fault detection method for detecting rolling bearings of wind turbines called VMD-AMCKD. This method combines complementary advantages of VMD and adaptive maximum correlated kurtosis deconvolution (AMCKD). At the same time, the Grasshopper optimization algorithm (GOA) is adapted to adaptively select the key parameters in MCKD. The experiment show that the method has strong stability. Cui *et al.* [22] proposed a fault feature extraction method based on parallel double Q factor and improved MCKD. The method firstly uses the parallel double Q factor to sparsely decompose the fault signal to obtain the resonance component of the signal, and the fault signal is filtered and de-noised by the proposed method. The results show that the method effectively avoids mutual interference between fault components. However, MCKD cannot extract continuous pulse signals, which makes fault feature extraction inaccurate, this shortcoming limits its development. In order to overcome the shortcomings of MED and MCKD, the method of Multi-point Optimal Adjustment of Minimum Entropy Deconvolution (MOMEDA) [23] was proposed. The purpose of this algorithm is to deconvolve continuous pulses by multi-point kurtosis, however, MOMEDA can only search for a single period of pulses each time in a certain time interval [24]. In addition, under the environment of strong noise, the periodic pulse searched by MOMEDA may be false component. At the same time, the fault period needs to be evaluated before using MOMEDA to process signals, the purpose is to reduce the noise reduction range as much as possible so as to improve the diagnostic accuracy. These shortcomings limit its development.

This paper has proposed a novel bearing fault detection method about adaptive Sparse-spike Deconvolution based on Curvelet Transform (CTSSD), where the novel technique about adaptive Sparse-spike Deconvolution names after ASSD. The purpose of ASSD is to recover the pulse sequence from a vibration signal including complex noise [25], and to evaluate the periodic pulse position and pulse amplitude. In this process, this paper proposes the L1 norm regularization method [26] to sparsely constrain the signal pulse sequence, so that its results are sparse and improves the stability of the result. But considering that regularization parameters are not adaptive. Therefore, the composite multi-scale dispersion entropy is selected as the fitness function in this paper. Then, the Quantum-behavior Particle Swarm Optimization (QPSO) algorithm is used for iterative operation to determine the optimal regularization parameters. Finally, considering the periodic features of ASSD extraction are not continuous, and the Curvelet transform is further introduced. The fault signal is transformed into the Curvelet domain, and the Curvelet coefficient is used to characterize the fault signal pulse sequence.

In recent years, due to the continuous development of intelligent algorithms, they have been widely used in parameter optimization. The Quantum-behaved Particle Swarm Optimization Algorithm [27] (QPSO) is a novel swarm intelligence optimization algorithm. The evolutionary equation of this algorithm is completely different from that of Particle Swarm Optimization (PSO), it has no velocity vector and is a completely random iterative equation, which overcomes many defects of PSO algorithm. Yi *et al.* [28] proposed an optimization method for operating parameters of aluminum electrolysis process based on improved quantum behavior particle swarm optimization algorithm. First, the aluminum electrolysis process (AEP) operating parameter optimization is formulated as a constrained multi-objective optimization problem. Then, the improved multi-objective quantum-behaved particle swarm optimization (IMQPSO) algorithm is proposed to optimize the parameters. Experiments verify the effectiveness of the method. Li *et al.* [29] proposed the prediction of atmospheric pollutant concentration based on support vector regression and quantum behavioral particle swarm optimization. The compared with PSO, QPSO algorithm has been tested more effectively in the process of parameter selection, which improves the global search ability and robustness.

The main contributions of this paper are as follows: (1) This paper presents a novel adaptive Sparse-spike Deconvolution (ASSD) which applies to fault diagnosis of rolling bearing. (2) In the process of ASSD processing fault signal, the L1 norm regularization parameter β is not adaptive. Therefore, the algorithm of QPSO is introduced to optimize the regularized parameter β. (3) Considering that the periodic features of ASSD extraction are not continuous, the Curvelet transform is further introduced. The fault signal is transformed into the Curvelet domain, and the Curvelet coefficient is used to characterize the fault signal pulse sequence.

II. SPARSE SPIKE DECONVOLUTION PRINCIPLE

In the bearing fault diagnosis, the vibration signal model can be expressed as:

$$d_t = w_t{}^* r_t + n_t \quad t = 1, 2, \ldots, N \tag{1}$$

The matrix form of equation (1) is (2)

$$d = wr + n \tag{2}$$

where d_t represents the vibration signal, w_t represents the transfer function, r_t represents the impact sequence, and n_t represents the noise. The purpose of SSD is to find a filter to recover the original shock signal r_t in the output d_t. According to equation (1), r_t can be considered as a highly ill-conditioned inverse problem. The specific process is as follows:

Calculate the error between the actual output and the expected output:

$$e_t = \sum_i w_{t-i} r_i - d_t \quad i = 1, 2, \ldots, N \tag{3}$$

According to formula (4), the error is constrained by the least square to ensure that the solution tends to the true solution.

$$J_r = \sum_i \frac{1}{2} e^2 \tag{4}$$

Define the objective function J, so that the objective function J is minimized when r_t satisfies the condition.

$$J = J_r + \beta J_x \tag{5}$$

Among them, J_x is the regularization term and β is the regularization parameter. However, the choice of β is difficult, when β is chosen properly, its solution is accurate and sparse. In section B, the simulation signals are used to illustrate the influence of regularization parameters on sparse spike deconvolution, which verifies the necessity of optimizing regularization parameters. In this paper, the regularization parameters are optimized by using the QPSO algorithm, and the composite multiscale dispersion entropy is selected as the objective function of QPSO algorithm.

In paper, the L1 norm regularization method is proposed to sparsely constrain the signal pulse sequence, so that the result is the sparse and the stability of the solution is improved. The following analysis of regularization constraint method.

A. REGULARIZATION CONSTRAINT

Solving r_t according to equation (1) can be considered as a highly ill-conditioned inverse problem. In order to solve this inverse problem, it is necessary to find a method to correct the it, so that the it can overcome its own uncertainty, this method is called regularization method. At present, due to L2 regularization method has strong practicability and good effectiveness, L2 norm regularization method has become the preferred method for scientific researchers to solve highly ill-conditioned inverse problems. However, when the solution x is sparse, the sparsity of solution x cannot be reflected by using the L2 norm regularization method. At the same time, the solution x obtained by L2 norm regularization method is quite different from the real solution. So, in order to make the result more accurate and sparse, this paper uses L1 norm regularization to constrain the pulse sequences. The model of L1 norm regularization in this paper is as follows:

$$J_x = \sum_i |r_t| \tag{6}$$

The new objective function can be defined as follows:

$$J = \sum_i \frac{1}{2} e^2 + \beta \sum_i |r_t| \tag{7}$$

In order to obtain r_t satisfying conditions, formula (6) can be minimized according to formula (8).

$$\partial J / \partial r_i = \sum\nolimits_t e_t w_{t-i} + \beta \sum\nolimits_i |r_i| / r_i = 0 \tag{8}$$

The formula (9) can be derived from the above formula.

$$\sum\nolimits_t \sum\nolimits_i \left[\left(w_{t-i}\, w_{t-i} + \beta\ 1 / |r_i| \right) r_i \right] = \sum\nolimits_t \left(w_{t-i} d_t \right) \tag{9}$$

Transform formula (9) into matrix form is:

$$(R + Q)x = g \tag{10}$$

Among them, $Q = diag(\beta / |r_i|)$, $diag$ represents that the column vector is transformed into the corresponding diagonal matrix; x represents that the column vector of the pulse sequence r_i.

The solution of SSD is an iterative process, the paper proposes an adaptive linear least squares iteration to obtain a high-precision signal pulse sequence to evaluate the periodic pulse position and pulse amplitude. The iteration stops when the expected error or the customized maximum iteration number $it_{\max}$ is reached. The main process is as follows:

(1) Set the parameter β of L1 norm regularization.

(2) Calculate the matrices R and g.

(3) Using the conventional deconvolution result A, the initial matrix B is calculated according to equation (11).

$$Q^{(0)} = diag(\beta / |x_s|) \tag{11}$$

(4) Calculate $x^{(k)}$ and $Q^{(k)}$ according to the following formula:

$$\begin{cases} x^{(k)} = (R + Q^{(k-1)})^{-1} g \\ Q^{(k)} = diag(\beta / \left| x^{(k)} \right|) \end{cases} \tag{12}$$

Among them, k is the number of iterations.

(5) When the maximum number of iterations is reached, the iteration is stopped.

B. THE INFLUENCE OF REGULARIZATION PARAMETERS ON SSD

The selection of regularization parameters is very important for solving highly ill-conditioned inverse problems. When the regularization parameters are selected properly, its solution is accurate and sparse. The following simulation signals were constructed to verify the necessity of optimizing regularization parameters.

$$x\,(t) = x_1\,(t) + noise \tag{13}$$

The composition signal $x_1\,(t) = A_m \times \exp(-g / T_m) \sin(2\pi f_c t)$.

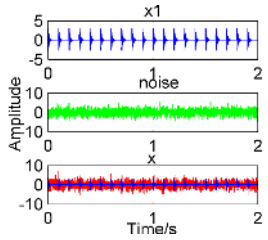

FIGURE 1. Simulation signal.

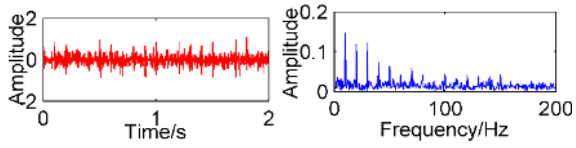

(a) (b)

When the value of the regularization parameter β is 3.

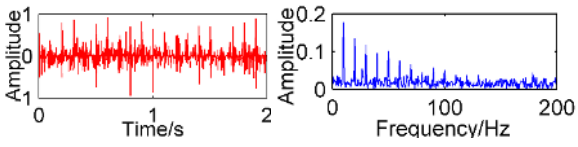

(a) (b)

When the value of the regularization parameter β is 5.

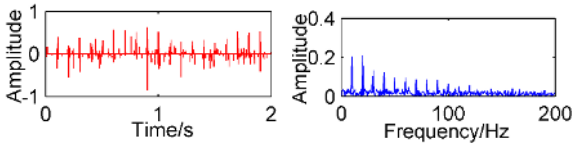

(a) (b)

When the value of the regularization parameter β is 8.

FIGURE 2. Influence of different regularization parameters on sparse spike deconvolution results, (a) is the time domain diagram, (b) is the corresponding envelope spectrum.

$x_1(t)$ is a periodic impact signal, which is specifically used to simulate the failure of the rolling bearing.

A_m represents the impact amplitude, and value of A_m is 2.5;

g is the damping coefficient, and value of g is 0.1;

T_m is the impact period, and value of T_m is 0.1, the failure period is 10Hz;

f_c is the rotation frequency of the bearing, and value of f_c is 280Hz;

The composition signal $noise = A \times randn(n)$ is the noise signal, and the value of A is 0.7.

The signal is shown in Figure 1. In Figure 2, if the value of the regularization parameters is set too small, such as $\beta = 3$, the highly ill-conditioned inverse problem will be not improved well, and the result of solution is still unstable. If the value of the regularization parameter is set too large, such as $\beta = 8$, an unideal approximate solution, which make the solution often deviates seriously from the ideal solution, cannot reach the expected result. Therefore, the selection of optimal regularization parameters can prevent the occurrence of the above two cases.

C. QPSO ALGORITHM OPTIMIZES REGULARIZATION PARAMETERS

QPSO algorithm is a population intelligent algorithm based on the PSO algorithm, this algorithm gets rid of the limitation of traditional speed-displacement orbital model, and the Monte Carlo algorithm is used to locate the updated particles, which make the algorithm more intelligent.

QPSO is improved particle swarm optimization algorithm based on quantum mechanics, which has the advantages of fast convergence, high robustness, strong global optimization ability and no special requirements on objective function. At the same time, QPSO algorithm has strong global search ability and can converge to the global optimal solution.

In quantum space, it is impossible to determine the position and velocity of particles at the same time. Therefore, we need to use a wave function $\psi(x, t)$ to represent the state of the particle, and the potential well model of particle swarm is established, the probability density function Q (Y) of the particle is:

$$\psi(Y) = 1/\sqrt{L}e^{-2|Y|/L} \tag{14}$$

$$Q(Y) = |\psi(Y)|^2 = 1/Le^{-2|Y|/L} \tag{15}$$

Among them, $L = 1/\beta = h^2/m\gamma$ is the characteristic length of the particle swarm potential well, m is the mass of the particle; h is the Planck constant.

The particle probability distribution function F(Y) is:

$$F(Y) = 1 - e^{-2|Y|/L} \tag{16}$$

In order to describe the precise position of particles in the search space in QPSO algorithm, the Monte Carlo simulation of the equation is used to transform the quantum state of the particle into the traditional state to measure the particle position. The particles move around the P point under the action of the potential well, and through evolution, its position equation is expressed as:

$$x = p \pm L/2 \ln 1/u \tag{17}$$

Among them $L = 1/\beta = h^2/m\gamma$ is the characteristic length of the particle swarm potential well. u is the uniformly distributed random number on the interval (0,1). Equation (17) is the basic evolution equation of QPSO algorithm.

In N-dimensional space, the convergence of QPSO algorithm is that the flight path of the particle gradually converges to its attractor. If the total number of particles in the population is M, each particle is N-dimensional, then the attractor of the i-th particle is $p_i = (p_{i,1}, p_{i,1}, \ldots, p_{i,N})$ and the coordinate is:

$$p_{i,j}(t) = \varphi_{i,j}(t) p_{i,j}(t) + [1 - \varphi_{i,j}(t)] G_j(t) \tag{18}$$

$$\varphi_{i,j}(t) = c_1 r_{1,i,j}(t) / [c_1 r_{1,i,j}(t) + c_2 r_{2,i,j}(t)] \tag{19}$$

Which, when $c_1 = c_2$, $\varphi_j(t)$ a random number on (0,1), $p_{i,j}(t)$ is individual optimal position of the t-th particle i, $G_j(t)$ is the global optimal position for the t-th particle.

The potential well is constructed for the particle with attractor $p_{i,j}$ as the center. According to formula (14), the wave function of particle i is:

$$\psi\left(x_{i,j}\left(t+1\right)\right)=1\Big/\sqrt{L_{i,j}\left(t\right)}\exp\left[\frac{-\left|x_{i,j}\left(t+1\right)-p_{i,j}\left(t\right)\right|}{L_{i,j}\left(t\right)}\right] \tag{20}$$

The probability density function of particle i is:

$$\begin{aligned} Q\left(x_{i,j}\left(t+1\right)\right) &= \left|\psi\left(x_{i,j}\left(t+1\right)\right)\right|^2 \\ &= 1\Big/\sqrt{L_{i,j}\left(t\right)}\exp\left[-2\left|x_{i,j}\left(t+1\right)\right.\right. \\ &\quad \left.\left.-p_{i,j}\left(t\right)\right|\Big/L_{i,j}\left(t\right)\right] \end{aligned} \tag{21}$$

The probability distribution function of particle i is:

$$F\left(x_{i,j}\left(t+1\right)\right)=1-\exp\left[\frac{-2\left|x_{i,j}\left(t+1\right)-p_{i,j}\left(t\right)\right|}{L_{i,j}\left(t\right)}\right] \tag{22}$$

According to equation (17), the evolution equation of the j-th dimension of particle i is:

$$x_{i,j}\left(t+1\right)=p_{i,j}\left(t\right)\pm L_{i,j}\left(t\right)\Big/2\ln 1\Big/u_{i,j} \tag{23}$$

Among them, $u_{i,j}\sim U(0,1)$. According to equation (23), if the particle swarm can converge to the local attractor p_i, $L_{i,j}\left(t\right)$ must be controlled so that it converges to 0, $L_{i,j}\left(t\right)$ can be evaluated by equation (24):

$$L_{i,j}\left(t\right)=2a\left|C_j\left(t\right)-x_{i,j}\left(t\right)\right| \tag{24}$$

In the formula, $C_j\left(t\right)$ is the average individual optimal position, and $C_j\left(t\right)$ is introduced for the algorithm of QPSO to better converge to the global optimal, the formula is as follows:

$$\begin{aligned} C_j\left(t\right) &= \left[C_1\left(t\right),C_2\left(t\right),\ldots,\ C_N\left(t\right)\right] \\ &= \left[1\Big/M\sum_{i=1}^{M}p_{i,1}\left(t\right),1\Big/M\sum_{i=2}^{M}p_{i,2}\left(t\right),\ldots,\right. \\ &\quad \left.1\Big/M\sum_{i=N}^{M}p_{i,N}\left(t\right)\right] \end{aligned} \tag{25}$$

Then the evolution equation of the particle is:

$$x_{i,j}\left(t+1\right)=p_{i,j}\left(t\right)\pm a\left|C_j\left(t\right)-x_{i,j}\left(t\right)\right|\ln 1\Big/u_{i,j} \tag{26}$$

In the formula, a is the coefficient of contraction and expansion, whose value determines the convergence speed of the algorithm. In order to make the algorithm have better convergence results, its value is generally linearly reduced from 1.0 to 0.5.

The $\pm$ in the evolution equation is determined by random number $u_{i,j}$, When $u_{i,j}<0.5$, take the "+"sign, when $u_{i,j}\geq 0.5$, take the "-"sign.

The basic process of QPSO algorithm is as follows:

Set the dimension of the solution space is N. In the solution space, quantum particle swarm consists of the M solution particles, the composition of the particle form is $x\left(t\right)=\left[x_1\left(t\right),x_2\left(t\right),\ldots,x_M\left(t\right)\right]$. The position of the i-th particle is:

$$x_i\left(t\right)=\left[x_{i,1}\left(t\right),x_{i,2}\left(t\right),\ldots,x_{i,N}\left(t\right)\right]\quad i=1,2,\ldots,M \tag{27}$$

In a particle swarm, the best position of each individual particle is:

$$p_i\left(t\right)=\left[p_{i,1}\left(t\right),p_{i,2}\left(t\right),\ldots,p_{i,N}\left(t\right)\right] \tag{28}$$

The global best position of the group is:

$$G\left(t\right)=\left[G_1\left(t\right),XG_2\left(t\right),\ldots,G_M\left(t\right)\right] \tag{29}$$

Among them, $p_i\left(t\right)=G_g\left(t\right)$, g is the subscript of the particle at the global best position, $g\in\{1,2,\ldots,M\}$.

For minimization problem $\min_{x\in s}f\left(x\right)$, the smaller the fitness value of the particle, it represents that the better the candidate solution. The individual best position (pbest) of particle i is determined by equation (30).

$$p_i\left(t\right)=\begin{cases} x_i\left(t\right) & f\left[x_i\left(t\right)\right]\geq f\left[x_i\left(t\right)\right] \\ p_i\left(t-1\right) & f\left[x_i\left(t\right)\right]\geq f\left[x_i\left(t\right)\right] \end{cases} \tag{30}$$

The global best position (gbest) of quantum particle swarm is determined by equations (30) and (31).

$$\begin{cases} g=\arg\min\limits_{1<i<M}\left\{f\left[p_i\left(t\right)\right]\right\} \\ G\left(t\right)=p_g\left(t\right) \end{cases} \tag{31}$$

$$\begin{cases} p_{i,j}\left(t\right)=\varphi_j\left(t\right)p_{i,j}\left(t\right)+\left[1-p_{i,j}\left(t\right)\right].G_i\left(t\right) \\ \varphi_j\left(t\right)=U\left(0,1\right) \end{cases} \tag{32}$$

Then the evolution equation of the particle is:

$$\begin{cases} x_{i,j}\left(t+1\right)=p_{i,j}\left(t\right)\pm\alpha\left|C_j\left(t\right)-x_{i,j}\left(t\right)\right|\Big/\ln 1\Big/u_{i,j} \\ u_{i,j}=U\left(0,1\right) \end{cases} \tag{33}$$

Among them,

$$C_j\left(t\right)=1\Big/M\sum_{i=2}^{M}p_{i,j}\left(t\right) \tag{34}$$

In this paper, the composite multiscale dispersion entropy(CMDE)is selected as the objective function of QPSO algorithm to optimize the regularization parameter. The composite multiscale dispersion entropy theory is as follows:

The DE algorithm is based on the mapping of the normal distribution function. There are two parameters: the average value μ and the standard deviation σ of the data to be analyzed. In the CMDE algorithm, when calculating the DE value of the composite coarse-grained multiscale sequence, both μ and σ are Based on raw data, not coarse-grained sequences.

The CMDE calculation steps are as follows:

(1) For the initial time series $\{u(i),i=1,2,\ldots,L\}$, When the scale factor is τ, the KTH coarse granulation order is listed

as $x_k^\tau = \left\{x_{k,1}^{(\tau)}, x_{k,1}^{(\tau)}, \ldots\right\}$ Known by the following formula:

$$x_{k,j}^\tau = \frac{1}{\tau} \sum_{i=k+\tau(j-1)}^{k+j\tau-1} u_i, \quad 1 \le j \le L/\tau \tag{35}$$

Then: $1 \le k \le \tau$.

(2) The CMDE under each scale factor τ is defined as:

$$CMDE(X, m, c, d, \tau) = \frac{1}{\tau} \sum_{i=k+\tau(j-1)}^{\tau} u_i, \quad 1 \le j \le L/\tau \tag{36}$$

In the formula: DE represents the calculation of the distribution entropy, the parameters m, c and d are the embedding dimension, category and delay in DE, respectively. See the literature for the calculation process of DE.

D. THE QPSO ALGORITHM OPTIMIZES REGULARIZATION PARAMETER AS FOLLOWS

Step1: Determine the parameters of the quantum particle swarm. Such as dimension, size W and the maximum number of iterations.

Step2: Set t = 0, and initialize each particle of quantum particle swarm in M-dimensional solution space, randomly obtain the spatial position x_i (0) of each particle, and initialize the individual best position of each particle to p_i (0) = x_i (0).

Step3: According to equation (34), the quantum particle swarm mbest is obtained.

Step4: Perform steps 5-8 for each particle*i*.

Step5: Calculate the fitness value of the current position x_i (t) of particle i, and pbest of particle is updated according to equation (30). The update method is to compare the fitness value of the current x_i (t) with the current fitness value of p_i ($t-1$), if the fitness value of x_i (t) is better than the fitness value of the p_i ($t-1$), that is, f [x_i (t)] < f [p_i ($t-1$)]. Then set p_i (t) = x_i (t). Otherwise p_i (t) = p_i ($t-1$).

Step6: For particle i, we need to compare its fitness value of p_i (t) with the current fitness value of G ($t-1$), if the fitness value of the p_i (t) is better than the fitness value of the G ($t-1$), that is, f [p_i (t)] < f [G ($t-1$)], then set p_i (t) = G (t). Otherwise G (t) = G ($t-1$)

Step7: According to equation (32), the random positions of each particle in the particle swarm can be obtained.

Step8: Update the latest position of the particle according to equation (33).

Step9: For whether to stop the iteration, if the termination condition is satisfied, the iteration is terminated. If the termination condition is not satisfied, then t = t + 1 and returns step 2.

The specific flow chart of the proposed method is as follows:

Sparse-spike deconvolution uses the quantum behavior particle swarm optimization algorithm to optimize the regularization parameters, and extracts part of the signal pulse sequence. However, more impact components are lost in the whole deconvolution process. As a result, the extracted shock signal is not complete. This process will not only lead to misdiagnosis, but also not easy to find the location of the fault. So a novel adaptive Sparse-spike deconvolution based on Curvelet transform is proposed in this paper. In theory, the Curvelet transform has the best sparse representation of fault signal and can obtain the best nonlinear approximation. According to the different distribution characteristics of the effective signal and random noise in the Curvelet domain, the continuity of the signal pulse sequence can be realized, and ensure the integrity of the signal. The further improve the accuracy of the method proposed in this paper to deal with bearing fault signals.

III. NOVEL SPARSE SPIKE DECONVOLUTION BASED ON CURVELET TRANSFORM (CTSSD)

A. THE CURVELET TRANSFORMATION PRINCIPLE

The Curvelet transform [32], [33] is implemented by the inner product of the Curvelet basis function and the objective function. In order to construct the Curvelet basis function, first, the two window functions are introduced. In the space, assuming that the spatial domain variable is x, the frequency domain variable is w, and the polar coordinates are r and θ, the radius window $W(r)$ and the angle window $V(t)$ are introduced, both of which satisfy the allowable conditions:

$$\sum_{j=-\infty}^{\infty} W^2(2^j r) = 1 r \in (3/4, 3/2) \tag{37}$$

$$\sum_{j=-\infty}^{\infty} V^2(t-l) = 1 t \in (-1/2, 1/2) \tag{38}$$

For all $j_0 \le j$, According to the Fourier transform, the frequency window U_jc can be defined as:

$$U_j(r, \theta) = 2^{-3j/4} W(2^{-j} r) V\left(2^{[j/2]}/2\pi\right) \tag{39}$$

where $[j/2]$ is the integer part of $j/2$. $\varphi_j(x)$ is defined as the basis function of the Curvelet, its Fourier form is $\hat{\varphi}_j(w) = U_j(w)$, then other 2^{-j}-scale Curvelet basis functions can be obtained by the rotation and translation of the basis function $\varphi_j(x)$. Define the rotation angle to $\theta_l = 2\pi \cdot 2^{-[j/2]} \cdot l$, $l = 0, 1, \ldots, 0 \le \theta_l \le 2\pi$; The translation parameter is $k = (k_1, k_2) \in z^2$, The Curvelet basis function at scale 2^{-j}, direction θ_l, and position $x_k^{(j,l)} = R_{\theta_l}^{-1}\left(k_1 \cdot 2^{-j}, k_2 \cdot 2^{-j/2}\right)$ is defined as:

$$\varphi_{i,l,k}(x) = \varphi_j\left[R_{\theta_l}\left(x - x_k^{(j,l)}\right)\right] \tag{40}$$

where $R_\theta = \begin{pmatrix} \cos\theta & \sin\theta \\ -\sin\theta & \cos\theta \end{pmatrix}$ represents the rotation of θ radians and R_θ^{-1} represents the inverse of R_θ, that is $R_\theta^{-1} = R_\theta^T = R_\theta$.

After the Curvelet base function of the $f(x) \in L^2(R^2)$ function, the $L^2(R^2)$-tight frame can be obtained by rotation and translation, and its reconstruction formula is:

$$f(x) = \sum_{j,l,k} \left[f(x), \varphi_{j,l,k}\right] \varphi_{j,l,k} \tag{41}$$

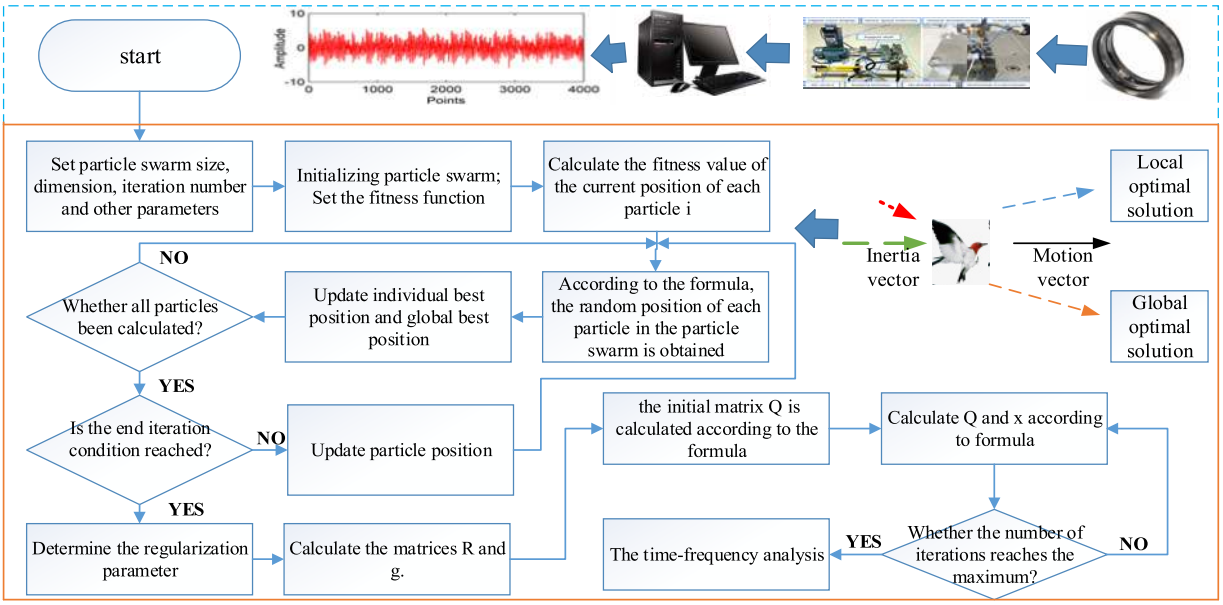

FIGURE 3. L1 norm regularization parameter optimization flow chart.

Since the scaling factors of the radius window and the angle window are not uniform during rotation and translation, in the time domain, when the dimension is j, the expansion scale of radius window is 2^{-j}, and the expansion scale of angle window is $2^{-j/2}$.

B. NOVEL SPARSE-SPIKE DECONVOLUTION BASED ON CURVELET TRANSFORM (CTSSD)

Although the ASSD extracts the pulse sequence of the partial fault signal, more impact components are lost during the entire deconvolution process, causes the extracted shock signal to be incomplete and misdiagnosed. Therefore, this paper proposes a novel adaptive sparse-spike deconvolution based on Curvelet transform, which overcomes the shortcomings of ASSD and further improves the accuracy of the proposed method in dealing with bearing fault signals.

Introducing the Curvelet transform operator C in equation (2), then

$$d = wr + n = wC^T x_c + n \tag{42}$$

where x_c is the Curvelet coefficient of the signal r, and C^T is the inverse transform of the Curvelet, that is $r = C^T x_c$.

In this paper, the bearing fault signal is transformed into Curvelet domain, and the pulse sequence is represented by Curvelet coefficient. The formula is expressed as:

$$\begin{cases} x_1 = \arg\min_x \|x_c\|_1 \\ r = C^T x_1 \end{cases} \tag{43}$$

where r is the pulse sequence of the bearing fault signal; C^T is the inverse Curvelet transform operator, and x_1 is the Curvelet coefficient vector. Equation (43) represents solving a set of sparse Curvelet coefficients that are the smallest in the sense of a set of L1 norms.

The constrained optimal problem of equation (43) can be solved by the unconstrained optimization problem equation (44).

$$x_1 = \arg\min \frac{1}{2} \left\| d - wC^T x_c \right\|_2 + \lambda \|x_c\|_1 \tag{44}$$

where λ is the tradeoff parameter and the value of the tradeoff parameter λ is critical. If the value of λ is too large, the loss of the Curvelet coefficient corresponding to the effective signal in the bearing fault signal, so that the impulse signal extracted by the method proposed in this paper has no integrity; If the value of R is too small, the random noise in the bearing fault signal will be residual, which will result in misdiagnosis. Therefore, the method for selecting the λ value in this paper is: Solving the optimization problem of equation (19) by gradually decreasing the value of λ from a large λ value, when the optimal solution of equation (19) satisfies $\left\| d - wC^T x \right\| \approx \varepsilon$, the value of λ is the optimal value.

$$x_c = T_\lambda \left(x_c + \left(wC^T \right)^T \left(Y - wC^T x_c \right) \right) \tag{45}$$

where T_λ represents a soft threshold function and T represents a conjugate operator.

$$T_\lambda (x_c) = sgn (x_c) \cdot \max (0, |x_c| - |\lambda|) \tag{46}$$

Loop iteration once, λ value decreases once. The Curvelet coefficients are iteratively updated through threshold iterations to obtain a fault signal sequence with high accuracy.

The specific solution steps are as follows:

Step1: First initialize a set of zero value Curvelet coefficients, set the c value, select the number of iterations M;

Step2: The bearing fault signal d is $\left(wC^T \right)^T$ transformed to obtain the initial Curvelet coefficient C_c;

Step3: To obtain x_c^t by $\left(wC^T \right)^T$ transformation of x_c in (1);

Step4: The coefficient of Curvelet is $x_c = C_c - x_c^t$, and the cycle iteration is M times;

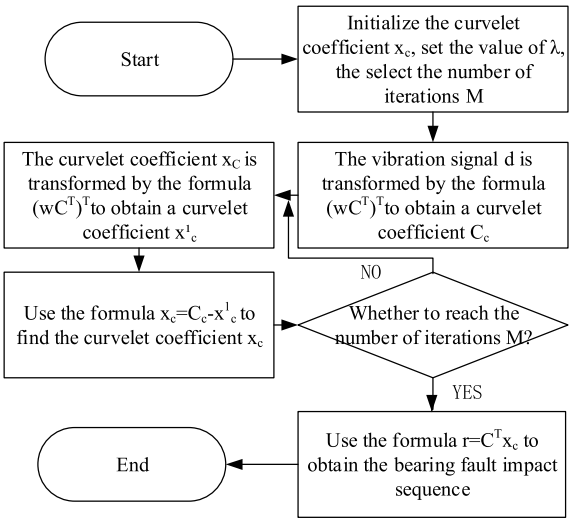

FIGURE 4. Novel sparse-spike deconvolution flow chart based on Curvelet transform.

Step5: Threshold processing of x_c according to equation (46);

Step6: According to a certain step size, reduces the value of λ, and repeats the process of steps Step3 to Step6;

Step7: Finally, the impact sequence of the fault signal is obtained by the formula $r = C^T x_c$.

IV. APPLICATION OF THE METHOD PROPOSED IN THIS PAPER IN BEARING FAILURE

A. TESTING USING SIMULATION SIGNALS

In order to illustrate the effectiveness of ASSD in signal processing, this paper uses the simulation signal of bearing fault to analyze in the strong noise environment. The simulation signal model is shown in equation (13).

The simulation signal waveform is shown in figure 1. It can be seen that the amplitude of the noise is larger than amplitude of the pulse, and the pulse is drowned by the noise.

In this paper, QPSO is used to search the regularization parameters of SSD. It can be known from the reference [27], the parameters of QPSO are set is: the number of particles 40, number of iterations n = 20. In QPSO algorithm, the composite multiscale dispersion entropy is selected as the fitness function. In order to make the noise reduced signal highlight more effective continuous periods, the composite multiscale dispersion entropy is as small as possible. Due to the minimum value of fitness function appears in the sixth generation, and its fitness value is 7.093, so the corresponding regularization optimal parameter is 7.217.

In order to verify the reliability and effectiveness of the proposed method, this section will use ASSD, MED and CTSSD to process the above rolling bearing fault simulation signals, the analysis results are shown in figure 5, figure 6 and figure 7. The simulation signal is processed by ASSD, and the results are shown in figure 5. Figure 5 (a) shows the time domain diagram after ASSD process signal, it can be seen that the ASSD extracts part of the pulse signal, but loses more impact components during the entire deconvolution process, resulting in the extracted impact signal not having integrity;

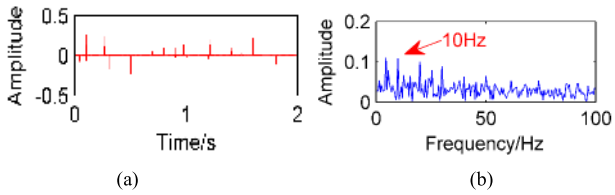

FIGURE 5. ASSD deals with simulation signal (a) is the time domain diagram (b) is the corresponding envelope spectrum.

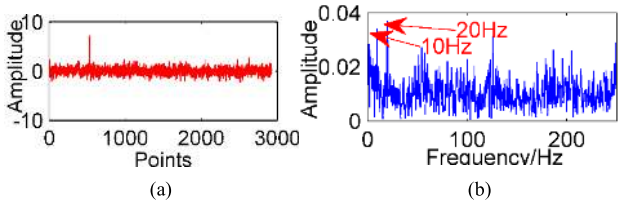

FIGURE 6. MED deals with simulation signal (a) is the time domain diagram (b) is the corresponding envelope spectrum.

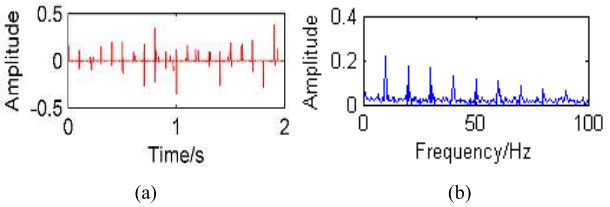

FIGURE 7. CTSSD deals with simulation signal (a) is the time domain diagram (b) is the corresponding envelope spectrum.

Figure 5 (b) is the corresponding envelope spectrum, it can be seen from the envelope spectrum that the fault frequency period cannot be accurately extracted.

It can be known from the reference [30], set a parameter of MED is: L = 68, the simulation signal is processed by MED are shown in figure 6. Figure 6 (a) is the time domain waveform diagram after MED process signal, it can be seen that there is no obvious periodic shock in the time domain diagram, and the time domain waveform is disorderly, and there is still a lot of noise. Figure 6 (b) is the corresponding envelope spectrum, it can be seen that there is a failure frequency period of 10Hz and its double frequency 20Hz, and the surrounding is covered with many useless noise spectral lines, which cannot accurately extract the fault frequency period. Therefore, the MED cannot effectively reduce signal noise and highlights its periodicity in the environment of strong noise.

The simulation signal is processed by CTSSD, and the results are shown in figure 7. Figure 7 (a) shows the time domain diagram after CTSSD process signal. It shows that the pulse signal extracted by CTSSD has strong periodicity, and the noise reduction effect of CTSSD is obvious; Figure 7 (b) is the corresponding envelope spectrum. It shows from the envelope spectrum that the fault frequency and its frequency doubling are obvious.

B. TEST WITH EXPERIMENTAL SIGNALS

In order to verify the feasibility and superiority of the adaptive SSD in engineering application. Test bearing type is

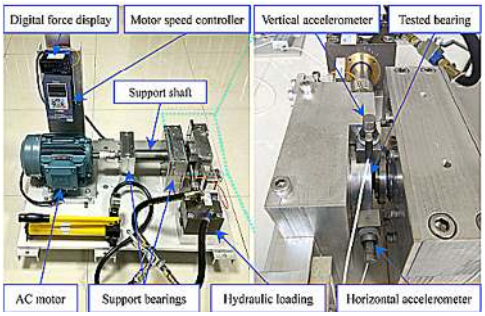

FIGURE 8. Rolling bearing test bed.

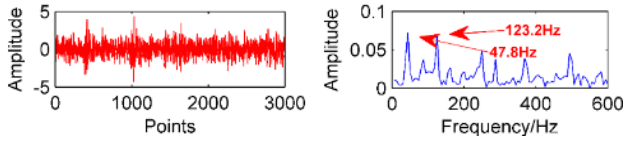

FIGURE 9. Fault signal of outer ring of rolling bearing (a) is the time domain diagram (b) is the corresponding envelope spectrum.

LDK UER204 [31], it is provided by the Institute of Design Science and Basic Component at Xi,an Jiaotong University, Shanxi and the Changxing Sumyoung Technology Co., Ltd. Its parameters are: Bearing mean diameter D = 34.55mm, ball diameter D_1 = 7.92mm, ball number n = 8, the shaft speed n_1 = 2400, sampling point 4096, sampling frequency 25600Hz. According to the calculation, the outer ring fault characteristic frequency is f = 123.2Hz. The bearing test bed shown in Figure 8 is composed of an alternating current (AC) induction motor, a motor speed controller, a support shaft, two support bearings (heavy duty roller bearings), a hydraulic loading system and so on. The accelerated degradation tests of rolling element bearings conduct in this test bed under different operating conditions (that is, different radial force and rotating speed). The hydraulic loading system generates the radial force applied to the housing of tested bearings. The speed controller of AC induction motor sets and keeps the rotating speed.

Figure 9 shows the outer ring fault signal of the rolling bearing. It can be seen that the amplitude of the noise is greater than the amplitude of the outer ring fault signal, and the fault signal of the outer ring is drowned by the noise. The corresponding envelope spectrum is 47.8 Hz and 123.2 Hz, so the fault frequency cannot be accurately determined. Therefore, the fault signal needs further noise reduction processing.

In this paper, QPSO is used to search the regularization parameters of ASSD. The parameters of QPSO are set is: the number of particles 40, number of iterations n = 100. In QPSO algorithm, the composite multiscale dispersion entropy is selected as the fitness function. In order to make the noise reduced signal highlight more effective continuous periods, the composite multiscale dispersion entropy is as small as possible. The minimum value of fitness function appears in the sixth generation, and its fitness value is

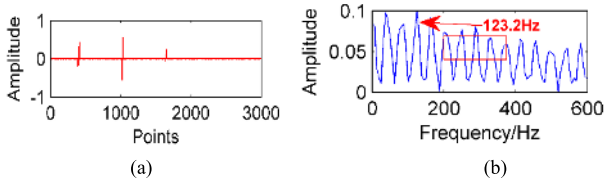

FIGURE 10. ASSD deals with the failure signal of the outer ring of rolling bearing (a) is the time domain diagram (b) is the corresponding envelope spectrum.

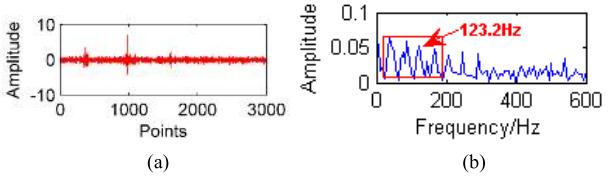

FIGURE 11. MED deals with the failure signal of the outer ring of rolling bearing (a) is the time domain diagram (b) is the corresponding envelope spectrum.

7.790, so the corresponding regularization optimal parameter is 7.8214.

The ASSD is used to process the outer ring fault signal of the rolling bearing, and the result is shown in figure 10. Figure 10 (a) shows the time domain diagram after ASSD process signal. It shows that the ASSD extracts part of the pulse signal, but loses more impact components during the entire deconvolution process, resulting in the extracted impact signal not having integrity; Figure 10 (b) is the corresponding envelope spectrum, it can be seen from the envelope spectrum that the fault frequency period is 123.2Hz. However, the fault frequency is covered with useless noise lines, and the fault frequency period cannot be accurately extracted, resulting in misdiagnosis.

It can be known from the reference [30], set the parameters of MED is: L = 346. The fault signal of rolling bearing outer ring is processed by MED; the result is shown in figure 11. Figure 11(a) shows the time-domain waveform diagram after the EMD processes the fault signal. It can be seen that there is no obvious periodic shock in the time domain diagram, and the time domain waveform is disorganized, there is still a lot of noise, the noise reduction effect of MED is not obvious. Figure 11 (b) shows the corresponding envelope spectrum, it can be seen that the failure frequency period is 123.2Hz and there's a lot of noise frequency around, so the failure frequency cannot be accurately extracted by MED the processing signal. Therefore, in the environment of strong noise, MED cannot effectively reduce signal noise and can't highlight its periodicity. Obviously, when processing signals, the method proposed in this paper is obviously superior to MED.

The CTSSD is used to process the outer ring fault signal of the rolling bearing, and the result is shown in figure 12. Figure 12 (a) shows the time domain diagram after CTSSD process signal. It can be seen that rolling bearing fault signal extracted by CTSSD has periodicity. In addition, the noise reduction effect is obvious. Figure 12 (b) is the corresponding

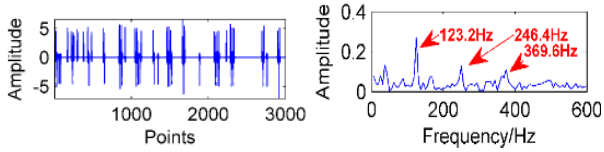

FIGURE 12. CTSSD deals with the failure signal of the outer ring of rolling bearing (a) is the time domain diagram (b) is the corresponding envelope spectrum.

envelope spectrum. It can be clearly seen from the envelope spectrum that the fault frequency is 123.2Hz, the frequency doubling is 246.4Hz, and the 3 times frequency is 369.6Hz. At the same time, the fault frequency is obvious. Therefore, the CTSSD is better than the ASSD and the MED in dealing with rolling bearing fault signals.

V. CONCLUSION

(1) This paper proposes an adaptive technology ASSD for fault diagnosis. However, in the process of processing the fault signal by the ASSD, since the L1 norm regularization parameter β is not adaptive, the sparsity and stability of the solution are not ideal, which seriously affects the result of the ASSD processing fault signal. Therefore, the quantum behavior particle swarm optimization algorithm is introduced to optimize the regularization parameter β.

(2) This paper proposes a novel bearing fault detection method about adaptive Sparse-spike Deconvolution based on Curvelet Transform (CTSSD). In this paper, the ASSD is analyzed by using the rolling bearing fault simulation signal and experimental signal. It is found that the ASSD extracts part of the pulse signal, but loses more impact components during the entire deconvolution process, resulting in the extracted impact signal not having integrity, causing misdiagnosis. Therefore, in this paper, Curvelet transform is introduced to transform the fault signal into the Curvelet domain, and the Curvelet coefficient is used to characterize the fault signal pulse sequence. This method proposed in this paper is applied to simulation signal and vibration signal of rolling bearing fault, and it is compared with the ASSD and the minimum entropy deconvolution (MED) to verify the reliability and effectiveness.

REFERENCES

[1] Z. Huang, Z. Wang, and L. Liu, "A practical fault diagnosis algorithm based on aperiodic corrected-second low-frequency processing for microgrid inverter," *IEEE Trans. Ind. Informat.*, vol. 15, no. 7, pp. 3889–3898, Jul. 2019.

[2] N. Liu, L. He, X. Yu, and L. Ma, "Multiparty energy management for grid-connected microgrids with heat-and electricity-coupled demand response," *IEEE Trans. Ind. Informat.*, vol. 14, no. 5, pp. 1887–1897, May 2018.

[3] K. Zhong, M. Han, T. Qiu, and B. Han, "Fault diagnosis of complex processes using sparse kernel local Fisher discriminant analysis," *IEEE Trans. Neural Netw. Learn. Syst.*, vol. 31, no. 5, pp. 1581–1591, May 2020.

[4] P. Sangeetha B. and H. S., "Rational-dilation wavelet transform based torque estimation from acoustic signals for fault diagnosis in a three-phase induction motor," *IEEE Trans. Ind. Informat.*, vol. 15, no. 6, pp. 3492–3501, Jun. 2019.

[5] X. Deng, X. Tian, S. Chen, and C. J. Harris, "Nonlinear process fault diagnosis based on serial principal component analysis," *IEEE Trans. Neural Netw. Learn. Syst.*, vol. 29, no. 3, pp. 560–572, Mar. 2018.

[6] C. Keliris, M. M. Polycarpou, and T. Parisini, "An integrated learning and filtering approach for fault diagnosis of a class of nonlinear dynamical systems," *IEEE Trans. Neural Netw. Learn. Syst.*, vol. 28, no. 4, pp. 988–1004, Apr. 2017.

[7] T. de Bruin, K. Verbert, and R. Babuska, "Railway track circuit fault diagnosis using recurrent neural networks," *IEEE Trans. Neural Netw. Learn. Syst.*, vol. 28, no. 3, pp. 523–533, Mar. 2017.

[8] S. Lu, Q. He, and J. Wang, "A review of stochastic resonance in rotating machine fault detection," *Mech. Syst. Signal Process.*, vol. 116, pp. 230–260, Feb. 2019.

[9] Z.-X. Yang, X. Wang, and P. K. Wong, "Single and simultaneous fault diagnosis with application to a multistage gearbox: A versatile dual-ELM network approach," *IEEE Trans. Ind. Informat.*, vol. 14, no. 12, pp. 5245–5255, Dec. 2018.

[10] Y. Li, M. Xu, Y. Wei, and W. Huang, "A new rolling bearing fault diagnosis method based on multiscale permutation entropy and improved support vector machine based binary tree," *Measurement*, vol. 77, pp. 80–94, Jan. 2016.

[11] Z. Wang, J. Wang, W. Cai, J. Zhou, W. Du, J. Wang, G. He, and H. He, "Application of an improved ensemble local mean decomposition method for gearbox composite fault diagnosis," *Complexity*, vol. 2019, May 2019, Art. no. 1564243, doi: 10.1155/2019/1564243.

[12] Z. Wang, L. Zheng, W. Du, W. Cai, J. Zhou, J. Wang, X. Han, and G. He, "A novel method for intelligent fault diagnosis of bearing based on capsule neural network," *Complexity*, vol. 2019, pp. 1–17, Jun. 2019, doi: 10.1155/2019/6943234.

[13] Z. Du, X. Chen, H. Zhang, and B. Yang, "Compressed-sensing-based periodic impulsive feature detection for wind turbine systems," *IEEE Trans. Ind. Informat.*, vol. 13, no. 6, pp. 2933–2945, Dec. 2017.

[14] Z. Du, X. Chen, H. Zhang, R. Yan, and W. Yin, "Learning collaborative sparsity structure via nonconvex optimization for feature recognition," *IEEE Trans. Ind. Informat.*, vol. 14, no. 10, pp. 4417–4430, Oct. 2018.

[15] Z. Feng, X. Chen, and M. J. Zuo, "Induction motor stator current AM-FM model and demodulation analysis for planetary gearbox fault diagnosis," *IEEE Trans. Ind. Informat.*, vol. 15, no. 4, pp. 2386–2394, Apr. 2019.

[16] H. Endo and R. B. Randall, "Enhancement of autoregressive model based gear tooth fault detection technique by the use of minimum entropy deconvolution filter," *Mech. Syst. Signal Process.*, vol. 21, no. 2, pp. 906–919, Feb. 2007.

[17] Z. Wang, G. He, W. Du, J. Zhou, X. Han, J. Wang, H. He, X. Guo, J. Wang, and Y. Kou, "Application of parameter optimized variational mode decomposition method in fault diagnosis of gearbox," *IEEE Access*, vol. 7, pp. 44871–44882, 2019.

[18] H. Liu and J. Xiang, "A strategy using variational mode decomposition, L-kurtosis and minimum entropy deconvolution to detect mechanical faults," *IEEE Access*, vol. 7, pp. 70564–70573, 2019.

[19] Z. Wang, J. Zhou, J. Wang, W. Du, J. Wang, X. Han, and G. He, "A novel fault diagnosis method of gearbox based on maximum kurtosis spectral entropy deconvolution," *IEEE Access*, vol. 7, pp. 29520–29532, 2019.

[20] Y. Miao, M. Zhao, J. Lin, and Y. Lei, "Application of an improved maximum correlated kurtosis deconvolution method for fault diagnosis of rolling element bearings," *Mech. Syst. Signal Process.*, vol. 92, pp. 173–195, Aug. 2017.

[21] J. Zhang, J. Zhang, M. Zhong, J. Zhong, J. Zheng, and L. Yao, "Detection for incipient damages of wind turbine rolling bearing based on VMD-AMCKD method," *IEEE Access*, vol. 7, pp. 67944–67959, 2019.

[22] Cui, Du, Yang, Xu, and Song, "Compound faults feature extraction for rolling bearings based on parallel Dual-Q-Factors and the improved maximum correlated kurtosis deconvolution," *Appl. Sci.*, vol. 9, no. 8, p. 1681, Apr. 2019.

[23] G. L. McDonald and Q. Zhao, "Multipoint optimal minimum entropy deconvolution and convolution fix: Application to vibration fault detection," *Mech. Syst. Signal Process.*, vol. 82, pp. 461–477, Jan. 2017.

[24] Z. Wang, W. Du, J. Wang, J. Zhou, X. Han, Z. Zhang, and L. Huang, "Research and application of improved adaptive MOMEDA fault diagnosis method," *Measurement*, vol. 140, pp. 63–75, Jul. 2019.

[25] D. R. Velis, "Stochastic sparse-spike deconvolution," *Geophysics*, vol. 73, no. 1, pp. R1–R9, Jan. 2008.

[26] R. Fernandes, H. Lopes, and M. Gattass, "Lobbes: An algorithm for sparse-spike deconvolution," *IEEE Geosci. Remote Sens. Lett.*, vol. 14, no. 12, pp. 2240–2244, Dec. 2017.

[27] J. Sun, W. Fang, X. Wu, V. Palade, and W. Xu, "Quantum-behaved particle swarm optimization: Analysis of individual particle behavior and parameter selection," *Evol. Comput.*, vol. 20, no. 3, pp. 349–393, Sep. 2012.

[28] J. Yi, J. Bai, W. Zhou, H. He, and L. Yao, "Operating parameters optimization for the aluminum electrolysis process using an improved quantum-behaved particle swarm algorithm," *IEEE Trans. Ind. Informat.*, vol. 14, no. 8, pp. 3405–3415, Aug. 2018.
[29] X. Li, A. Luo, J. Li, and Y. Li, "Air pollutant concentration forecast based on support vector regression and quantum-behaved particle swarm optimization," *Environ. Model. Assessment*, vol. 24, no. 2, pp. 205–222, Apr. 2019.
[30] J. Li, M. Li, and J. Zhang, "Rolling bearing fault diagnosis based on time-delayed feedback monostable stochastic resonance and adaptive minimum entropy deconvolution," *J. Sound Vib.*, vol. 401, pp. 139–151, Aug. 2017.
[31] B. Wang, Y. Lei, N. Li, and N. Li, "A hybrid prognostics approach for estimating remaining useful life of rolling element bearings," *IEEE Trans. Rel.*, vol. 69, no. 1, pp. 401–412, Mar. 2020, doi: 10.1109/TR.2018.2882682.
[32] N. Eslahi and A. Aghagolzadeh, "Compressive sensing image restoration using adaptive curvelet thresholding and nonlocal sparse regularization," *IEEE Trans. Image Process.*, vol. 25, no. 7, pp. 3126–3140, Jul. 2016.
[33] P. Hill, A. Achim, M. E. Al-Mualla, and D. Bull, "Contrast sensitivity of the wavelet, dual tree complex wavelet, curvelet, and steerable pyramid transforms," *IEEE Trans. Image Process.*, vol. 25, no. 6, pp. 2739–2751, Jun. 2016.

YANFENG LI was born in Taiyuan, Shanxi, China, in 1990. He received the bachelor's degree in engineering from the University of Jinan, in 2014, and the master's degree in engineering from the Taiyuan University of Technology, in 2017, where he is currently pursuing the Ph.D. degree with the College of Mechanical and Vehicle Engineering.

From 2014 to 2019, he was committed to the fault diagnosis research of rotating machinery. He participated in a number of National Natural Science Foundation of China. He has been responsible for the design and analysis of experiments and has written reports on them. He has published a number of research articles.

Dr. Li was awarded the Doctoral Scholarship in 2018 and 2019.

ZHIJIAN WANG was born in Zhengzhou, Henan, in 1985. He received the Ph.D. degree in engineering from the Taiyuan University of Technology, in 2015. He is currently pursuing the Ph.D. degree with Xi'an Jiaotong University.

He is currently an Associate Professor and a Master Supervisor with the School of Mechanical Engineering, North University of China. He has presided the National Natural Science Foundation of China and the Natural Science Foundation of Shanxi Province. Since 2015, he has published more than 40 academic articles, among which the first author or corresponding author has published more than 20 SCI articles related to the subject, two articles cited by ESI, and seven articles included by EI, and has authorized four patents and more than 20 national invention patents applied by the first inventor and one monograph.

Dr. Wang is a review expert of international famous SCI journals, such as *ISA Transactions*, *Measurement*, *Journal of Vibration and Control*, and IEEE Access.

TIANSHENG ZHAO was born in China, in 1978. He received the bachelor's degree in industrial automation from East China Jiaotong University, in 2001. He is currently a Senior Engineer with the Zhengzhou Mechanical and Electrical Engineering Research Institute. His research interests include mechanical and electrical control and fault diagnosis technology. He has won one first prize and one second prize from China Shipbuilding Industry Corporation Science and Technology Award.

YUAN ZHAO received the Ph.D. degree from the Taiyuan University of Technology, Taiyuan, China, in 2019. In 2020, he entered Taiyuan Research Institute Company Ltd., China Coal Technology and Engineering Group, where he holds a postdoctoral position. He currently works with Taiyuan Research Institute Company Ltd., China Coal Technology and Engineering Group, as an Associate Researcher. He was engaged in the design and development of trackless auxiliary transportation equipment.